

# Microscale 3D Collagen Cell Culture Assays in Conventional Flat-Bottom 384-Well Plates

Journal of Laboratory Automation  
1–8  
© 2014 Society for Laboratory  
Automation and Screening  
DOI: 10.1177/2211068214563793  
jala.sagepub.com  


Brendan M. Leung<sup>1\*</sup>, Christopher Moraes<sup>1,2\*</sup>, Stephen P. Cavnar<sup>1</sup>,  
Kathryn E. Luker<sup>3</sup>, Gary D. Luker<sup>1,3,4</sup>, and Shuichi Takayama<sup>1,5,6</sup>

## Abstract

Three-dimensional (3D) culture systems such as cell-laden hydrogels are superior to standard two-dimensional (2D) monolayer cultures for many drug-screening applications. However, their adoption into high-throughput screening (HTS) has been lagging, in part because of the difficulty of incorporating these culture formats into existing robotic liquid handling and imaging infrastructures. Dispensing cell-laden prepolymer solutions into 2D well plates is a potential solution but typically requires large volumes of reagents to avoid evaporation during polymerization, which (1) increases costs, (2) makes drug penetration variable and (3) complicates imaging. Here we describe a technique to efficiently produce 3D microgels using automated liquid-handling systems and standard, nonpatterned, flat-bottomed, 384-well plates. Sub-millimeter-diameter, cell-laden collagen gels are deposited on the bottom of a ~2.5 mm diameter microwell with no concerns about evaporation or meniscus effects at the edges of wells, using aqueous two-phase system patterning. The microscale cell-laden collagen-gel constructs are readily imaged and readily penetrated by drugs. The cytotoxicity of chemotherapeutics was monitored by bioluminescence and demonstrated that 3D cultures confer chemoresistance as compared with similar 2D cultures. Hence, these data demonstrate the importance of culturing cells in 3D to obtain realistic cellular responses. Overall, this system provides a simple and inexpensive method for integrating 3D culture capability into existing HTS infrastructure.

## Keywords

aqueous two-phase system, 3D culture, high-throughput screening

## Introduction

Conventional in vitro high-throughput screening (HTS) and high-content screening platforms have mostly been based on two-dimensional (2D) cell culture platforms because of their compatibility with robotics, liquid-handling systems, and imaging platforms. In parallel, three-dimensional (3D) culture platforms such as cell-laden hydrogels have gained much attention as alternative, and in many ways, more physiologically accurate culture models. Cells maintained in 3D culture display altered gene expression profiles,<sup>1,2</sup> metabolic functions,<sup>3–5</sup> sensitivities toward drugs,<sup>6,7</sup> and physical stimuli.<sup>8,9</sup> Despite these advantages, the adoption of 3D culture methods into industrial HTS platforms has been slow, partly because of the cumbersome hydrogel-handling techniques and challenges in maintenance, automated data collection, and analysis. The most straightforward approach to introducing 3D matrix in a cell-based assay is to embed cells in a hydrogel matrix. Common matrices used in 3D platforms include naturally derived extracellular matrix (ECM) proteins such as collagen, fibrin, and Matrigel. Collagen type I is the most abundant of these

<sup>1</sup>Department of Biomedical Engineering, Biointerfaces Institute, University of Michigan, Ann Arbor, MI, USA

<sup>2</sup>Department of Chemical Engineering, McGill University, Montreal, Canada

<sup>3</sup>Center for Molecular Imaging, Department of Radiology, University of Michigan Medical School, Ann Arbor, MI, USA

<sup>4</sup>Department of Microbiology and Immunology, University of Michigan Medical School, Ann Arbor, MI, USA

<sup>5</sup>Department of Macromolecular Science and Engineering, University of Michigan, Ann Arbor, MI, USA

<sup>6</sup>Division of Nano-Bio and Chemical Engineering WCU Project, UNIST, Republic of Korea

\*Equal contributors: B. M. Leung and C. Moraes

Received Aug 27, 2014.

Supplementary material for this article is available on the *Journal of Laboratory Automation* Web site at <http://jala.sagepub.com/supplemental>.

## Corresponding Author:

Shuichi Takayama, Department of Biomedical Engineering and Macromolecular Science and Engineering Program, Biointerfaces Institute, University of Michigan, 2800 Plymouth Rd, NCRC, Bldg 10 A183, Ann Arbor, MI 48109, USA.  
Email: [takayama@umich.edu](mailto:takayama@umich.edu)

ECMs found in the body<sup>10</sup> and would be valuable to incorporate into a 3D HTS format. Cell-laden collagen gels can be formed directly on nonpatterned culture dishes<sup>11</sup> but require large gel volumes (usually tens of microliters), and the throughput is low. Other methods such as tube casting of collagen modules<sup>12</sup> and microfluidic-based generation of collagen microbeads<sup>13</sup> can achieve much higher throughput but require specialized equipment and expertise and are not robust or mature enough technologies to support the demanding nature of HTS assays. Hence, adoption of these novel technologies into the HTS industry is limited. Ideally, techniques to generate low-volume collagen microgels in conventional HTS multiwell plates using existing robotic liquid-handling infrastructure would greatly aid adoption of 3D cultures in HTS industry.

Fabricating collagen gels at the microscale within a conventional multiwell plate can be challenging,<sup>14</sup> primarily because of evaporation during the thermal gelation process. Once extracted from its source, usually from rat tail or bovine skin, collagen is kept in solution and stored at low temperature and low pH to prevent gelation. Even for small volumes of material, neutralized collagen solution takes 30 to 40 min at 37 °C to completely gel. Microscale constructs in 384-well plates would need to be prepared with just a few microliters of collagen solution exacerbating this evaporation problem and significantly reducing the viability of any embedded cells.<sup>15</sup> Although evaporation may be minimized by tightly monitoring and controlling the atmospheric humidity during gelation, it would require specialized equipment and complicates its integration into the existing HTS infrastructure. The effects of evaporation can be partially alleviated by increasing the gel volume. However, the large wall surface area to internal volume ratio of a well in a 384-well plate would lead to the formation of significantly concaved meniscus, even with just tens of microliters of gel. Such curvature may lead to complications and optical interference during microscopy and other analysis modalities.

Here, we design a 3D culture solution that has been adapted for an automated 384-well plate format using a previously described method to fabricate collagen microgels in an aqueous two-phase system (ATPS).<sup>15</sup> Our ATPS system consists of two immiscible, phase-forming aqueous polymer solutions, poly(ethylene) glycol (PEG) and dextran (DEX). A 3D microgel is formed by adding collagen into the DEX phase and dispensing the mixture into a solution of PEG, where the collagen will partition to the interface and undergo thermal gelation to form a microgel. We characterized the size and morphology of the collagen microgel as a function of dispensing volume. The aqueous environment reduces evaporation-driven cell death and enables the formation of collagen microgels with volumes as small as 0.5  $\mu\text{L}$ . We also compared sensitivity to cytotoxic compounds between cells embedded in collagen microgels and cells seeded on a 2D surface using a bioluminescent assay.

## Materials and Methods

### Cell Culture

Breast ductal carcinoma cell line MDA-MB-231 expressing Click Beetle green luciferase CBG99 (Promega, Madison, WI) expressed from lentiviral vector FUW (gift of D. Baltimore), denoted here on as 231-LUC, was described in a previous study.<sup>16</sup> Cells were cultured at 37 °C in 5% CO<sub>2</sub> using Dulbecco's Modified Eagle's Medium (DMEM) (Invitrogen, Carlsbad, CA) supplemented with 10% fetal bovine serum and 1% antibiotic-antimycotic (Invitrogen). Cell stock were maintained in 100 mm plastic culture dishes until they reached ~80% confluence. For seeding and passaging, cells were washed with phosphate-buffered saline (PBS; Gibco) and then detached using 0.25% trypsin/EDTA (Gibco) and placed into the appropriate cell culture vessels.

### ATPS Collagen Microgel Printing in a 384-Well Plate

Collagen microgels were printed onto the floor of 384-well plates using the aqueous two-phase printing method. Briefly, stock solutions of DEX T500 (20% w/w DEX in PBS; DEX from Pharmacosmos, Holbaek, Denmark) and PEG (20% w/w in DMEM; PEG from Sigma, St. Louis, MO) were prepared as previously described.<sup>15</sup> Collagen-DEX solutions were prepared by diluting type I bovine collagen (BD Biosciences, San Jose, CA) to 2 mg mL<sup>-1</sup> in a sterile solution of 10% v/v 10 $\times$  DMEM, 1% v/v 3M NaOH, and 3% DEX in deionized water. This solution was kept on ice to prevent gelation. To prepare cell-laden collagen microgels in 384-well plates, 231-LUC cells were detached and mixed with collagen-DEX solution at a concentration of 10<sup>6</sup> cells/mL and loaded into a chilled 96-well round-bottom dispensing plate. A small volume (1–5  $\mu\text{L}$ ) of cell collagen-DEX mixture was dispensed into a clear, flat-bottom 384-well plate (No. 781098; Greiner Bio-One, Monroe, NC) containing 50  $\mu\text{L}$  of PEG (6% w/w) using a Cybi-Well 96-channel simultaneous pipettor (CyBio, Jena, Germany) fitted with sterile Cybi-TipTray 96 tips (25  $\mu\text{L}$ , #OL 3800-25-633-S). Liquid-handling routines were compiled and executed by CyBio Composer software (v2.13; CyBio). Dispensing height refers to the distance between the tip of the pipette to the bottom of the well. Two different heights, 0.5 mm and 2.5 mm, were tested for the delivery of cell-laden collagen-DEX solution into PEG. We also tested two dispensing speeds at high (10) and low (1) setting within the CyBio Composer. After dispensing the cell-laden collagen-DEX solution, the 384-well plates were then placed in an incubator for 30 min to allow the collagen to polymerize. Once gelation is complete, the wells were rinsed seven times with medium, each time replacing 25  $\mu\text{L}$ , which corresponds to 50% of the total liquid volume in each well.

This gives a theoretical dilution such that less than 1% of the original PEG remains. For the 2D culture system, cells were also seeded directly into the wells of the 384-well plate at the same cell-seeding density and using the same Cybi-Well setting as 3D collagen microgel.

### Chemotherapeutic Dose-Response Studies

The cytotoxic effects of three chemotherapeutics toward 231-LUC were compared between cells seeded in 2D culture and cells embedded in 3D collagen microgels. At 1 d postseeding, cells were treated with clinical formulations of cisplatin (NDC-0703-5748-11), paclitaxel (NDC-55390-304-50), and doxorubicin (NDC-0069-3030-20), from the University of Michigan Hospital Pharmacy. Drugs were added by replacing 25  $\mu\text{L}$  of medium with working solutions at  $2\times$  final concentrations. Appropriate series of concentrations spanning four orders of magnitude were chosen for each compound. Cell viability was assessed using a bioluminescence assay. After incubation for 2 d, the 384-well plates were rinsed three times with medium. For bioluminescence imaging, 25  $\mu\text{L}$  of a  $2\times$  working solution of luciferin (Promega) was added to each well, resulting in a final concentration of 1.5  $\mu\text{g}/\text{mL}$  luciferin. The plates were kept at room temperature and imaged after 30 min. Capture parameters including aperture, binning, and exposure time were adjusted so that the luminescence values falls between 9000 and 600 counts  $\text{s}^{-1}$ . Bioluminescence signals were collected using an IVIS Spectrum Imaging System (PerkinElmer, Waltham, MA; **Suppl. Fig. S4**). Data were acquired and analyzed using Living Image 4.0 (PerkinElmer). Signals from replicates ( $N=8$ ) were averaged, normalized against no-drug control, and plotted against the log of drug concentrations ( $\pm\text{SEM}$ ).

One experimental artifact that may cause such discrepancy between 2D and 3D responses may be the presence of detached cells that contain active luciferase and are readily rinsed away during the preluciferin assay wash in 2D rather than 3D culture. To rule out this possibility, we compared 2D culture with and without preluciferin assay rinse. The signals observed for the without-rinse samples were in close agreement with the rinsed control (**Suppl. Fig. S1**), suggesting negligible contribution of residual luciferase activity to the observed signals.

### Cytotoxicity of PEG and $Z'$ Factor of ATPS Collagen Microgel Bioluminescence Assay

To examine the cytotoxic effect of PEG 35K solutions, we incubated ATPS collagen microgel (1  $\mu\text{L}$ ) containing 1000 231-LUC cells in a series of half-diluted PEG 35K solutions. The final concentrations of PEG 35K used in the dose curve, in descending order, were 6.00%, 3.00%, 1.50%, 0.75%, 0.38%, 0.19%, 0.09%, 0.05%, 0.02%, and 0% (w/w). Viability was assessed after 2 d using a bioluminescence

assay as described in previous sections. We also took the bioluminescence readings at 0% and 1.5% PEG as negative and positive controls, respectively, to calculate the  $Z'$  factor of this assay. The  $Z'$  factor is a commonly used statistical parameter characterizing an HTS assay, which reflects both the signal dynamic range as well as data variations of signals. Because  $Z'$  uses data only from positive and negative controls, it is an assessment of the quality of the assay itself without intervention of drug candidate. Using a previously described formula,<sup>17</sup> the  $Z'$  factor can be calculated as follows:

$$Z' \text{ factor} = 1 - \frac{3s_h - 3s_l}{|\bar{X}_h - \bar{X}_l|}$$

where  $s$  is the standard deviation,  $\bar{X}$  is the average, and subscripts  $h$  and  $l$  represent positive and negative controls, respectively. The  $Z'$  factor calculated from these value is 0.83, indicating the assay quality is very good.<sup>17,18</sup>

### Mass Transport Simulations

Simulations of diffusion of molecules through collagen gels of various sizes were conducted in COMSOL v4.3 (Burlington, MA), using previously determined values for diffusion of large molecules in collagen-DEX (unpublished data). Diffusion coefficients for 0.1, 1, 10, and 100 kDa sized molecules were approximated using these data and the Einstein-Stokes relationship between hydrodynamic radius and diffusion. Diffusivity coefficients ranged from  $1.18 \times 10^{-9} \text{ m}^2/\text{s}$  for 0.1 kDa molecules to  $1.18 \times 10^{-10} \text{ m}^2/\text{s}$  for 100 kDa molecules. Geometric parameters for cylindrical collagen gels (in well plate), and hemispherical collagen gels (in ATPS) were estimated using previously published characterization data.<sup>15</sup> Simulations were set up such that the boundary of the hydrogel hemisphere was fixed at a finite concentration of the diffusing molecule, whereas the bulk of the hydrogel was initialized at a concentration of 0 ng/mL. Simulations report the equilibration fraction of the gel center as a function of time. This setup approximates the case of adding soluble factors to the well plate but neglects any delays that might occur due to diffusion of the soluble factor through the media surrounding the hydrogel. Because dispersion rates of molecules dispensed into water are typically at least an order of magnitude faster than diffusion through hydrogels, this delay should be negligible.

## Results and Discussion

### Characterization of ATPS Collagen Microgel

Previous studies from our group have demonstrated that collagen microgels can be fabricated in aqueous medium using ATPS.<sup>15</sup> In the current study, we adapt this technique

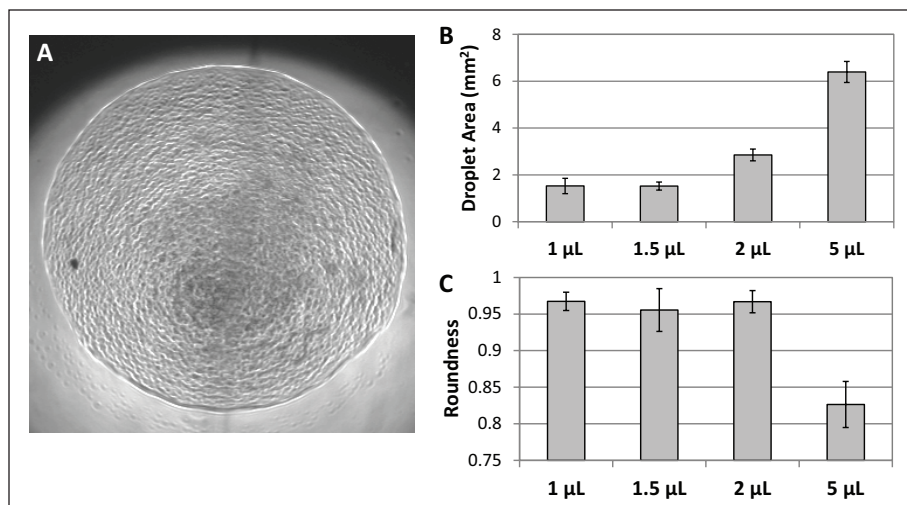


**Figure 1.** Physical characterization of collagen microgel. **(A)** Representative brightfield micrograph of a 1  $\mu\text{L}$  collagen microgel in 384-well plates (scale bar = 250  $\mu\text{m}$ ). **(B)** Microgel areas at different dispensing volumes. All subsequent experiments were performed using a 1  $\mu\text{L}$  microgel volume. **(C)** Microgels remain uniform and circular at a dispensing volume up to 2  $\mu\text{L}$ .

to create 3D cultures in 384-well format using robotic liquid-handling infrastructure, similar to that already available in existing commercial HTS equipment. Using the described collagen-ATPS formulations, we were able to form collagen microgels in 384-well plates. Similar to our previous observations,<sup>15</sup> collagen microgels deposited on the bottom of the well took on a circular morphology, and their sizes were proportional to printing volume (**Fig. 1A, B**). Collagen microgels also maintained good circularity, which began to diminish only at the higher printing volume of 5  $\mu\text{L}$  (**Fig. 1C**; **Suppl. Fig. S3**), suggesting that maintaining uniform culture conditions between wells in HTS would be facilitated by using highly reproducible low-volume droplets. In addition to printing volume, dispensing height may also affect microgel morphology. We tested two printing heights, at 0.5 mm and 2.5 mm above the bottom of the well. With our formulation, the lower dispensing height increased the likelihood of forming noncircular or satellite microgels; however, dispensing speed had no visible effect on microgel morphology (**Suppl. Fig. S2**). Maintaining similar morphologies between microgels in each well would help simplify automated imaging protocols. With optimized parameters (dispensing volume = 1  $\mu\text{L}$ , dispensing height = 2.5 mm, speed setting = 1), the yield of ATPS microgel printing was 100% for all the plates used in our experiments, and all the microgels remained attached to the bottom of the well. Overall, the robotic pipettor was able to deliver droplets with a high degree of accuracy and reproducibility in terms of shape and volume.

One of the advantages of using microgels instead of collagen macrogels is the reduction of equilibration time needed for small molecules to penetrate through the bulk of the gel. The long diffusion times for large molecules in 3D matrices may hinder transport of the test drug candidate to the cells encapsulated within the 3D matrix, and cells

located in the center of such gels may not even be stimulated by the drug of interest over the time course of the experiment.<sup>19</sup> To determine the impact of our microgels on alleviating this diffusion problem, we constructed finite element models to simulate diffusion of different size molecules, from 0.1 kDa to 100 kDa, into bulk collagen gel of 100  $\mu\text{L}$  in a 96-well and two ATPS collagen microgels of different volumes (10  $\mu\text{L}$  and 1  $\mu\text{L}$ ; **Fig. 2**). As expected, the models predict that the time it takes to equilibrate in 3D collagen gels is proportional to both the volume of the gel and the size of the molecule of interest. Small molecules including chemotherapeutics such as cisplatin (MW = 300 Da), doxorubicin (MW = 543 Da), and paclitaxel (MW = 854 Da) were able to penetrate and fully equilibrate in ATPS collagen microgels within 5 min, but in bulk collagen gel, complete saturation takes approximately 6 h. The small diffusion distance and high surface area-to-volume ratio of collagen microgels facilitate rapid saturation. This difference is magnified as the molecular weight increases. In our simulations, molecules weighing 1 to 100 kDa (a range that encompasses several growth factors including insulin, transforming growth factor- $\beta$ , and vascular endothelial growth factor) reached only 80% and 40% saturation concentration in bulk collagen macrogel after 4 h, respectively. In contrast, the increase in molecular weight posed only a modest delay in equilibration, and both the 1  $\mu\text{L}$  and 10  $\mu\text{L}$  microgels become completely equilibrated in less than 1 h. The simulations presented here demonstrate that the size of ATPS collagen microgel allows molecules with weights spanning a large range to diffuse rapidly and simultaneously to reach embedded cells. This can be a crucial feature in situations in which one needs to observe the combined effects of compounds with drastically different molecular weights or in a situation in which the experiment requires the complete removal or substitution of compound during

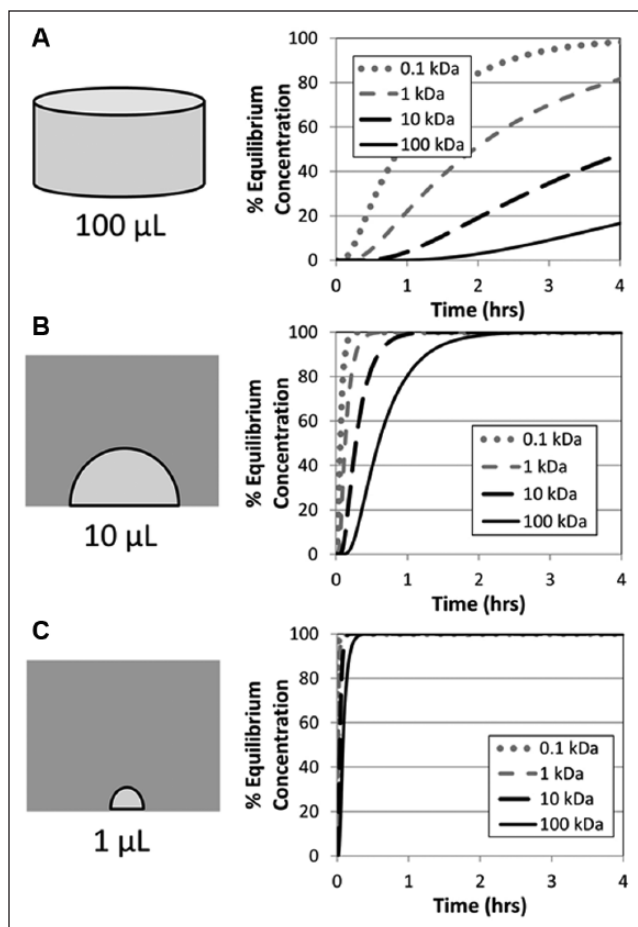


**Figure 2.** Finite element models showing percentage saturation of molecules of different weights as a function of time. For all geometry and volumes, the time required for complete saturation increases as the molecular weight of the compound increases. With the lowest surface area-to-volume ratio, conventional macrogel in a 96-well plate (A) presents a significant diffusion barrier to embedded cells. In contrast, the aqueous two-phase system collagen microgel, both large (B) and small (C), was able to reach saturation much more quickly.

the time course. In these experiments, the cell-seeding densities were significantly lower than that in densely packed tumor tissues or cell spheroids ( $<10^6$  cell/ $\mu\text{L}$ ). This is expected to allow for greater oxygen penetration depth and minimize hypoxic regions within the sub-millimeter-diameter microgel. Depending on application requirements, the method is flexible in terms of the cell-seeding density, and it should also be possible in the future to create higher cell density constructs if more hypoxic conditions are desired.

Although there is essentially no difference in cell-dispensing technique for seeding 384-well plates with conventional 2D cultures compared with our 3D collagen microgel assay, the presence of ATPS, specifically PEG, requires thorough washing to minimize cytotoxicity.<sup>15,20</sup> To avoid accidental removal or dislodgement of the collagen microgels, it is necessary to

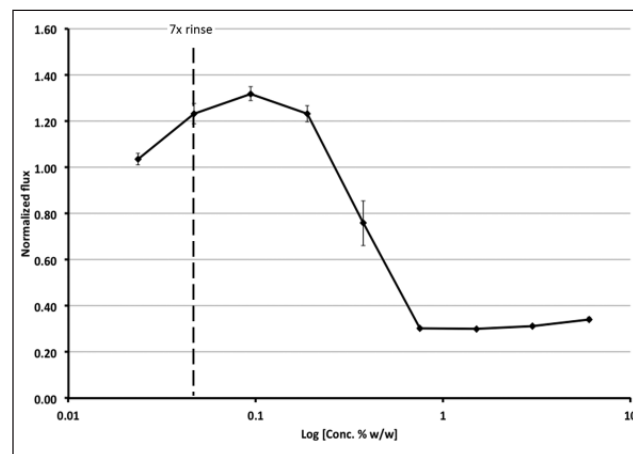


**Figure 3.** Cytotoxic effect of poly(ethylene) glycol (PEG) on 231-LUC cells embedded in aqueous two-phase system (ATPS) collagen microgel. Microgels were incubated in half-serial diluted PEG containing medium from 6% to 0.0234% w/w PEG 35K. After 2 d, cell viability was determined by bioluminescence assay and plotted against log[conc. PEG] ( $\pm$ SEM,  $N = 4$ ). Dashed line indicates the concentration of PEG (0.0468% w/w) after 7 $\times$  half-serial washes.

perform a series of half-volume sequential dilutions, with the pipettor set to withdraw at half the depth of the well (dispensing height = 5 mm) and dispense at the slowest speed (setting = 1). One of the concerns is that such a gentle rinse step would not be effective in removing the viscous PEG solution. To compensate for the poor rinsing efficiency, we performed this rinse cycle seven times over a total time of 20 min to ensure that the PEG would be sufficiently diluted to maintain cell viability. The number of rinses was chosen to yield a  $>99\%$  theoretical PEG removal efficiency, and the rinse time represents the minimum time required for the CyBi-Well to execute the serial dilution routine. Using the bioluminescence assay, we confirmed that our postrinsing protocol involving seven times half-volume serial rinse (theoretical final concentration of PEG 35K = 0.05% w/w) was sufficient to preserve the viability of 231-LUC cells embedded in collagen microgels (Fig. 3). Although fewer rinse steps may also be sufficient, for this proof-of-concept demonstration, this rinsing protocol was adopted in all subsequent experiments.

### Differential Responses to Chemotherapeutic between 2D and 3D Models

Beyond differences in mass transport kinetics, studies have also indicated that culturing cells in 3D matrix instead of 2D surfaces leads to alteration in cell phenotypes and function, including differentiation,<sup>21,22</sup> proliferation,<sup>23</sup> and survival.<sup>24</sup> For example, many tumor cells display reduced chemosensitivity in 3D cultures.<sup>25</sup> However, this increased resistance to chemotherapy may simply be due to increased

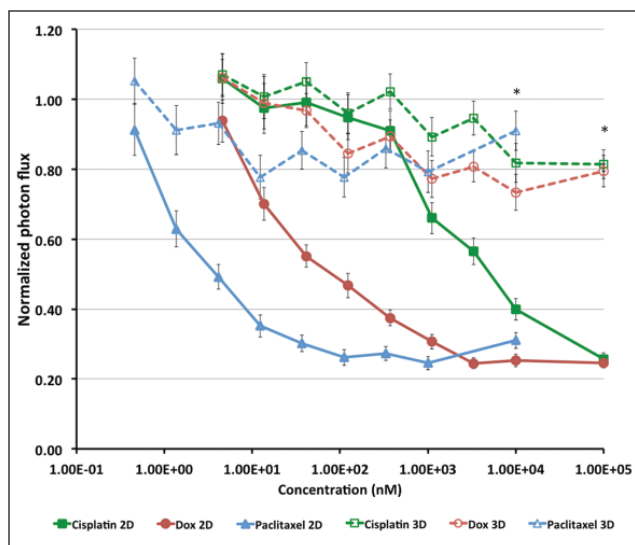


**Figure 4.** Bioluminescence-based cytotoxicity assay against three common chemotherapeutics (cisplatin, doxorubicin, and paclitaxel). Bioluminescences from MDA-MB-231 cells expressing Click Beetle Green luciferase (231-LUC) seeded in 384-well plates were measured using the IVIS Spectrum imager. Cells seeded in 3D collagen microgels showed increased chemoresistance to all three compounds compared with their 2D counterparts (\* $p < 0.005$ ,  $\pm$ SEM,  $N = 8$ ).

diffusion transport barriers between the drug and cells embedded in a bulk 3D matrix or protected by surrounding tumor cells, such as in a spheroid model system.<sup>26</sup> Hence, the impact of cell culture dimensionality alone remains unknown. Because our ATPS-microgel system enables culture of cells in microscale volumes of collagen, concerns over transport limitations can be eliminated. Moreover, culture of cells within 3D matrices that are attached to a surface enables the cells to generate tension within the matrix, without causing bulk matrix contraction, which in turn would alter the transport characteristics of the tissue. Cells that are allowed to generate tension can display a differential response toward growth factors,<sup>27,28</sup> as well as modulation of signaling networks.<sup>29</sup> Because cells in the body typically exist in matrices under tension, these features must be considered in the design of the in vitro drug-screening platform because the ultimate goal is to recapitulate the cellular responses in vivo and predict the outcome in the respective animal model.

Using bioluminescence assays, we compared the cytotoxic responses of mammary carcinoma cells expressing luciferase, 231-LUC, toward three commonly used chemotherapeutics, cisplatin, doxorubicin, and paclitaxel. Both cisplatin and doxorubicin exert their cytotoxic effects by intercalating and/or cross-linking DNA molecules, thus inhibiting mitosis and triggering apoptosis.<sup>30</sup> Paclitaxel operates by stabilizing microtubules during mitosis, thereby interfering with normal cell division.<sup>31</sup> Using the ATPS

collagen microgel technique, we seeded a 384-well plate in which each well contained a single 1  $\mu$ L microgel embedded with 1000 231-LUC cells. The cells were treated with a serial dilution of the aforementioned chemotherapeutics, and their viabilities were compared after 2 d against a 2D control plate, in which each well contained 1000 231-LUC cells seeding in culture medium. At the end of treatment, luciferin was added to each well, and the resulting bioluminescence was recorded (**Fig. 4A, B**). In 2D culture, cell viability decreased steadily as drug concentration increased, down to 20% to 30% at the highest concentrations compared with a no-drug control. In contrast, cell viability in 3D culture dropped to only approximately 80% of control for all three drugs even at the highest concentrations. Our data agree with previous findings,<sup>25,32,33</sup> in which cells cultured in 3D showed a substantial decrease in chemosensitivity, and clearly demonstrate that these effects are related to the dimensionality of the cell culture environment and not to transport limitations associated with conventional 3D cultures. Although uncovering the mechanism behind the differences in chemosensitivities between cells in 3D versus 2D is beyond the scope of this study, we believe that this difference may be caused by decreased cell proliferation in 3D systems,<sup>34</sup> thereby reducing drug uptake and activity.

### Performance and Advantages of the ATPS Collagen Microgel Platform

The quality and robustness of an assay is crucial in HTS applications because of the large number of test conditions and relatively small number of replicates. For this reason, the statistical parameter known as the  $Z'$  factor has been developed and widely adopted as a tool to assess the performance of HTS assays.<sup>17</sup> The  $Z'$  factor is calculated based on the values obtained from the positive and negative controls of the assay. Here we calculated the  $Z'$  factor for the ATPS collagen microgel cytotoxicity assay using bioluminescence values from 231-LUC cells at various concentrations of PEG (**Fig. 3**). The calculated  $Z'$  factor of 0.83 indicates that the assay is excellent with a large degree of confidence in identifying cytotoxic effects.

Aside from improved mass transport characteristics, the use of a small-volume collagen microgel also provides savings in both reagent costs and imaging time. When compared with conventional macrogel, a 1  $\mu$ L microgel platform provides a 100-fold reduction in collagen cost and cell number required per assay (**Table 1**). Simply pipetting a collagen solution into nonpatterned 384-well plates in an attempt to reduce collagen volume will cause most of the material to be lost in the corners of the well because of capillary action. Therefore, the use of ATPS provides a unique solution to easily create collagen microgels on ordinary culture surfaces by localizing collagen gel and reducing interfacial forces that can cause collagen drop wicking near the walls of the well.

**Table 1.** Cost and Analysis Time Comparison between Conventional Macrogel and Aqueous Two-Phase System Collagen Microgel.<sup>a</sup>

Number of Wells	100 $\mu$ L Macrogel in 96-Well Plate				1 $\mu$ L Microgel in 384-Well Plate			
	Cost of Collagen (\$)	Number of cells ( $10^6$ /mL)	z-Stack Height (mm)	z-Stack Scan Time	Cost of Collagen (\$)	Number of Cells ( $10^6$ /mL)	z-Stack Height (mm)	z-Stack Scan Time
1	1	$10^5$	3.13	6.3 s	0.01	$10^3$	0.78	1.5 s
$10^3$	1 thousand	$10^8$	3.13	1.73 h	10	$10^6$	0.78	25 min
$10^6$	1 million	$10^{11}$	3.13	72 days	10,000	$10^9$	0.78	18 d

<sup>a</sup>The cost of collagen was calculated based on the collagen solution used in this study. Z-stack scan time for confocal imaging was calculated based on 5  $\mu$ m optical slices and a scan time of 10 ms per slice.

Small volumes of collagen in microgels also reduces the overall height of the gel compared with collagen macrogel and therefore would significantly reduce the time needed for z-stack-based confocal imaging. For example, the estimated height of a hemispherical 1  $\mu$ L collagen microgel is 0.78 mm. In contrast, a 100  $\mu$ L collagen macrogel in 96 wells has a height of 3.13 mm, which represents a fourfold increase in z-stack height during confocal imaging. The smaller height of the microgel also means that the entire depth of the gel can be imaged by brightfield or epifluorescence microscopy using a low-magnification objective lens with low numerical aperture. Hence, the small size of the collagen microgel will also make this assay more easily compatible with a variety of microscopic techniques, including automated high-throughput imaging.

In this study, we employed ATPS patterning techniques to deliver cell-laden collagen microgels into 384-well plates using a common robotic liquid-handling system used for HTS. We found that collagen microgels take on a predictable size and morphology as a function of dispensing volume. Cells embedded in collagen microgels remain viable and, when compared with cells seeded on 2D surfaces, display significantly lower chemosensitivity. Our simulation also predicted that the small size of the ATPS collagen microgel enables rapid and simultaneous delivery of compound over a wide range of molecular weights. Technologically, the method described here provides a simple and inexpensive way to incorporate microscale 3D culture into existing HTS platforms. Compared with conventional macrogels, the small volume of ATPS collagen microgel can be more easily and rapidly analyzed with various imaging modalities and presents a significant saving in costs of materials. We believe the ATPS 3D collagen microgel culture system will be widely applicable to many HTS applications and represents a significant advancement in the field of microengineered culture platforms.

### Declaration of Conflicting Interests

S.T. owns stock in PHASIQ, Inc, a company commercializing related technology.

### Funding

The authors disclosed receipt of the following financial support for the research, authorship, and/or publication of this article: The authors would like to acknowledge funding support from the National Institutes of Health (CA170198) and the mCube grant from the University of Michigan. C.M. was supported by a Banting postdoctoral fellowship from the Natural Sciences and Engineering Research Council of Canada. S.C. was supported by a National Science Foundation predoctoral fellowship (F031543) and the Advanced Proteome informatics of Cancer Training Grant (T32 CA140044).

### References

- Kenny, P. A.; Lee, G. Y.; Myers, C. A.; et al. The Morphologies of Breast Cancer Cell Lines in Three-Dimensional Assays Correlate with Their Profiles of Gene Expression. *Mol. Oncol.* **2007**, *1*, 84–96.
- Kang, X.; Xie, Y.; Kniss, D. A. Adipose Tissue Model Using Three-Dimensional Cultivation of Preadipocytes Seeded onto Fibrous Polymer Scaffolds. *Tissue Eng.* **2005**, *11*, 458–468.
- Mehta, B. C.; Holman, D. W.; Grzybowski, D. M.; et al. Characterization of Arachnoidal Cells Cultured on Three-Dimensional Nonwoven PET Matrix. *Tissue Eng.* **2007**, *13*, 1269–1279.
- Bokhari, M.; Carnachan, R. J.; Cameron, N. R.; et al. Culture of HepG2 Liver Cells on Three Dimensional Polystyrene Scaffolds Enhances Cell Structure and Function during toxicological challenge. *J. Anat.* **2007**, *211*, 567–576.
- Sung, K. E.; Su, X.; Berthier, E.; et al. Understanding the Impact of 2D and 3D Fibroblast Cultures on In Vitro Breast Cancer Models. *PLoS One* **2013**, *8*, e76373.
- Millerot-Serruot, E.; et al. 3D collagen type I matrix inhibits the antimigratory effect of doxorubicin. *Cancer cell international* **2010**, *10*, 26.
- Kostadinova, R.; Boess, F.; Applegate, D.; et al. A Long-Term Three Dimensional Liver Co-Culture System for Improved Prediction of Clinically Relevant Drug-Induced Hepatotoxicity. *Toxicol. Appl. Pharmacol.* **2013**, *268*, 1–16.
- Storch, K.; Eke, I.; Borgmann, K.; et al. Three-Dimensional Cell Growth Confers Radioresistance by Chromatin Density Modification. *Cancer Res.* **2010**, *70*, 3925–3934.
- Shi, Z. D.; Abraham, G.; Tarbell, J. M. Shear Stress Modulation of Smooth Muscle Cell Marker Genes in 2-D and

- 3-D Depends on Mechanotransduction by Heparan Sulfate Proteoglycans and ERK1/2. *PLoS One* **2010**, *5*, e12196.
10. Karsenty, G.; Park, R. W. Regulation of Type I Collagen Genes Expression. *Int. Rev. Immunol.* **1995**, *12*, 177–185.
  11. Higashiyama, M.; Oda, K.; Okami, J.; et al. In Vitro-Chemosensitivity Test Using the Collagen Gel Droplet Embedded Culture Drug Test (CD-DST) for Malignant Pleural Mesothelioma: Possibility of Clinical Application. *Ann. Thorac. Cardiovasc. Surg.* **2008**, *14*, 355–362.
  12. McGuigan, A. P.; Leung, B.; Sefton, M. V. Fabrication of Cell-Containing Gel Modules to Assemble Modular Tissue-Engineered Constructs [erratum published in *Nat. Protoc.* 2006, *1*(6)]. *Nat. Protoc.* **2006**, *1*, 2963–2969.
  13. Matsunaga, Y. T.; Morimoto, Y.; Takeuchi, S. Molding Cell Beads for Rapid Construction of Macroscopic 3D Tissue Architecture. *Adv. Mater.* **2011**, *23*, H90–H94.
  14. Raghavan, S.; Shen, C. J.; Desai, R. A.; et al. Decoupling Diffusional from Dimensional Control of Signaling in 3D Culture Reveals a Role for Myosin in Tubulogenesis. *J. Cell Sci.* **2010**, *123*(pt 17), 2877–2883.
  15. Moraes, C.; Simon, A. B.; Putnam, A. J.; et al. Aqueous Two-Phase Printing of Cell-Containing Contractile Collagen Microgels. *Biomaterials* **2013**, *34*, 9623–9631.
  16. Coggins, N. L.; Trakimas, D.; Chang, S. L.; et al. CXCR7 Controls Competition for Recruitment of Beta-Arrestin 2 in Cells Expressing Both CXCR4 and CXCR7. *PLoS One* **2014**, *9*, e98328.
  17. Zhang, J. H.; Chung, T. D.; Oldenburg, K. R. A Simple Statistical Parameter for Use in Evaluation and Validation of High Throughput Screening Assays. *J. Biomol. Screen.* **1999**, *4*, 67–73.
  18. Birmingham, A.; Selfors, L. M.; Forster, T.; et al. Statistical Methods for Analysis of High-Throughput RNA Interference Screens. *Nat. Methods* **2009**, *6*, 569–575.
  19. Moraes, C.; Sun, Y.; Simmons, C. A. (Micro)Managing the Mechanical Microenvironment. *Integr. Biol.* **2011**, *3*, 959–971.
  20. Biondi, O.; Motta, S.; Mosesso, P. Low Molecular Weight Polyethylene Glycol Induces Chromosome Aberrations in Chinese Hamster Cells Cultured In Vitro. *Mutagenesis* **2002**, *17*, 261–264.
  21. Boukhechba, F.; Balaguer, T.; Michiels, J. F.; et al. Human Primary Osteocyte Differentiation in a 3D Culture System. *J. Bone Miner. Res.* **2009**, *24*, 1927–1935.
  22. Zhang, X.; Xie, Y.; Koh, C. G.; et al. A Novel 3-D Model for Cell Culture and Tissue Engineering. *Biomed. Microdev.* **2009**, *11*, 795–799.
  23. Ceresa, C. C.; Knox, A. J.; Johnson, S. R. Use of a Three-Dimensional Cell Culture Model to Study Airway Smooth Muscle-Mast Cell Interactions in Airway Remodeling. *Am. J. Physiol. Lung Cell Mol. Physiol.* **2009**, *296*, L1059–L1066.
  24. Li, C. L.; Tian, T.; Nan, K. J.; et al. Survival Advantages of Multicellular Spheroids vs. Monolayers of HepG2 Cells In Vitro. *Oncol. Rep.* **2008**, *20*, 1465–1471.
  25. Horning, J. L.; Sahoo, S. K.; Vijayaraghavalu, S.; et al. 3-D Tumor Model for In Vitro Evaluation of Anticancer Drugs. *Mol. Pharm.* **2008**, *5*, 849–862.
  26. Tung, Y. C.; Hsiao, A. Y.; Allen, S. G.; et al. High-Throughput 3D Spheroid Culture and Drug Testing Using a 384 Hanging Drop Array. *Analyst* **2011**, *136*, 473–478.
  27. Rhee, S.; Grinnell, F. Fibroblast Mechanics in 3D Collagen Matrices. *Adv. Drug Deliv. Rev.* **2007**, *59*, 1299–1305.
  28. Grinnell, F.; Ho, C. H.; Lin, Y. C.; et al. Differences in the Regulation of Fibroblast Contraction of Floating versus Stressed Collagen Matrices. *J. Biol. Chem.* **1999**, *274*, 918–923.
  29. Carlson, M. A.; Smith, L. M.; Cordes, C. M.; et al. Attachment-Regulated Signaling Networks in the Fibroblast-Populated 3D Collagen Matrix. *Sci. Rep.* **2013**, *3*, 1880.
  30. Siddik, Z. H. Cisplatin: Mode of Cytotoxic Action and Molecular Basis of Resistance. *Oncogene* **2003**, *22*, 7265–7279.
  31. Orr, G. A.; Verdier-Pinard, P.; McDaid, H.; et al. Mechanisms of Taxol Resistance Related to Microtubules. *Oncogene* **2003**, *22*, 7280–7295.
  32. Nirmalanandhan, V. S.; Duren, A.; Hendricks, P.; et al. Activity of Anticancer Agents in a Three-Dimensional Cell Culture Model. *Assay Drug Dev. Technol.* **2010**, *8*, 581–590.
  33. Loessner, D.; Stok, K. S.; Lutolf, M. P.; et al. Bioengineered 3D Platform to Explore Cell-ECM Interactions and Drug Resistance of Epithelial Ovarian Cancer Cells. *Biomaterials* **2010**, *31*, 8494–8506.
  34. Baker, B. M.; Chen, C. S. Deconstructing the Third Dimension: How 3D Culture Microenvironments Alter Cellular Cues. *J. Cell Sci.* **2012**, *125*(pt 13), 3015–3024.